Punctuated Aneuploidization of the Budding Yeast Genome

Lydia R. Heasley, Ruth A. Watson, and Juan Lucas Argueso[1]
Department of Environmental and Radiological Health Sciences, Colorado State University, Fort Collins, Colorado 80523
ORCID ID: 0000-0002-7157-1519 (J.L.A.)

ABSTRACT Remarkably complex patterns of aneuploidy have been observed in the genomes of many eukaryotic cell types, ranging from brewing yeasts to tumor cells. Such aberrant karyotypes are generally thought to take shape progressively over many generations, but evidence also suggests that genomes may undergo faster modes of evolution. Here, we used diploid *Saccharomyces cerevisiae* cells to investigate the dynamics with which aneuploidies arise. We found that cells selected for the loss of a single chromosome often acquired additional unselected aneuploidies concomitantly. The degrees to which these genomes were altered fell along a spectrum, ranging from simple events affecting just a single chromosome, to systemic events involving many. The striking complexity of karyotypes arising from systemic events, combined with the high frequency at which we detected them, demonstrates that cells can rapidly achieve highly altered genomic configurations during temporally restricted episodes of genomic instability.

KEYWORDS aneuploidy; genomic instability; punctuated evolution; genome evolution; copy number alteration variation

WHOLE chromosome copy number alterations (CCNAs) (*e.g.*, aneuploidies) are an important source of phenotypic variation and adaptive potential (Hickman *et al.* 2015; Selmecki *et al.* 2015; Sansregret and Swanton 2017; Forche *et al.* 2018; Gilchrist and Stelkens 2019). CCNAs usually arise from defects in chromosome segregation (Musacchio 2015), but, because such errors occur rarely ($\sim 10^{-6}$/cell/division) (Klein 2001; Kumaran *et al.* 2013), the patterns by which cells accumulate extensive collections of CCNAs remain poorly understood (Sansregret and Swanton 2017). Conventional paradigms of genome evolution posit that mutations (*e.g.*, CCNAs) are acquired gradually and independently over many successive generations (Nowell 1976; Podlaha *et al.* 2012). Cancer-centric models have proposed that tumor cells can gain numerous mutations during punctuated and transient bursts of genomic instability (Eldredge and Gould 1972; Gao *et al.* 2016; Sampaio *et al.* 2017; Field *et al.* 2018), or that they become chronically destabilized and acquire mutations at elevated rates (*i.e.*, mutator phenotype) (Loeb 2016; Coelho *et al.* 2019). Yet, because cancer genome evolution is retrospectively inferred many generations after neoplastic initiation, our understanding of how these mutagenic patterns contribute to the acquisition of CCNAs remains incomplete.

doi: https://doi.org/10.1534/genetics.120.303536
Manuscript received June 8, 2020; accepted for publication July 30, 2020; published Early Online August 4, 2020.
Available freely online through the author-supported open access option.
Supplemental material available at figshare: https://doi.org/10.25386/genetics.12749273.
[1]Corresponding author: Department of Environmental and Radiological Health Sciences, Colorado State University, 493 MRB Bldg., 1618 campus delivery, Fort Collins, CO 80523-1618. E-mail: lucas.argueso@colostate.edu

Results and Discussion

We used the tractable budding yeast model system to determine the patterns by which CCNAs arise. To recover aneuploid clones arising spontaneously from populations of diploid cells grown under normal culture conditions (*i.e.*, rich medium, 30C, <35 cell divisions), we introduced the counter-selectable marker *CAN1* onto the right arm of chromosome V (Chr5R) in the haploid strain JAY291 (Argueso *et al.* 2009). Because the endogenous copy resides on Chr5L, the resulting strain had two copies of *CAN1* on Chr5, one on each arm. We crossed this haploid to the S288c reference strain to form a heterozygous diploid. To select for cells that had lost the JAY291 homolog of Chr5 (jChr5), we grew independent cultures for ≤35 generations in rich medium and plated each onto selective medium containing canavanine (CAN) (Larimer *et al.* 1978). When we visually inspected CAN-resistant (CAN^R) colonies, we noted that while the majority had a normal smooth appearance; 1 in ~450 colonies displayed a

distinctive rough morphology (Figure 1A). Previously, we reported that this morphological switch is precipitated by interhomolog mitotic recombination (MR), resulting in loss of the wild-type allele of the *ACE2* gene encoded on sChr12R and homozygosis of the mutant *ace2-A7* allele on jChr12R (Rodrigues Prause *et al.* 2018). *ace2-A7* cells fail to separate after cytokinesis and consequently form rough colonies (Nelson *et al.* 2003; Rodrigues Prause *et al.* 2018). In this previous study, rough colonies appeared on nonselective media at a frequency of 1 in ~10,000 colonies, and were always caused by MR events spanning *ACE2* on Chr12R (Sampaio *et al.* 2017; Rodrigues Prause *et al.* 2018). Rough colonies resulting from complete loss of Chr12 were never observed (0/67 genotyped clones).

Our finding that rough colonies appeared >22-fold more frequently on CAN selection plates than in nonselective conditions led us to hypothesize that a shared mutational process could have caused the concomitant loss of jChr5 and loss-of-heterozygosity on Chr12R. To investigate this, we introduced a *URA3* marker onto sChr12L [Figure 1B, (1)]. Rough CAN^R clones resulting from MR spanning *ACE2* would likely retain this *URA3* marker and grow on medium lacking uracil (Ura^+) [Figure 1B, (2)], while rough clones caused by loss of the sChr12 homolog would be Ura^- [Figure 1B, (3)]. We plated cultures to CAN media, screened CAN^R colonies to identify rough clones, and determined the $Ura^{+/-}$ phenotype of each. In contrast to the rough colonies recovered from nonselective conditions (Sampaio *et al.* 2017; Rodrigues Prause *et al.* 2018), 79% (41/52) of rough CANR colonies had lost sChr12 in addition to jChr5 (Figure 1B). Our finding that the selected loss of jChr5 markedly shifted the mutational spectrum of LOH on Chr12R to CCNA was consistent with our above prediction, and indicated that clones harboring one aneuploidy were enriched for the presence of additional unselected aneuploidies.

We performed whole genome sequence (WGS) analysis to comprehensively define the genomic structure of 20 rough CAN^R Ura^- clones (Table S3). The even distribution of heterozygous sites across the genome of the S288c/JAY291 hybrid enabled us to detect CCNAs of each homolog and changes in overall ploidy based on sequencing read depth. Remarkably, the majority (65%) of the sequenced clones harbored unselected CCNAs of chromosomes other than jChr5 and sChr12 (Figure 1C and Table S3). Some clones had lost numerous chromosomes (LRH279), while others displayed systemic gains (LRH266 and LRH280) (Figure 1D). Intriguingly, one clone (LRH271) had acquired CCNAs of nearly every chromosome, such that both copies of one homolog had been retained while both copies of the other homolog had been lost—a state known as uniparental disomy (UPD) (Andersen and Petes 2012). As a result of this UPD-type CCNA, this clone had cumulatively gained and lost 32 homologs, and was fully homozygous for either parental haplotype of all chromosomes except Chr1, Chr3, and Chr9, which were tetrasomies (Figure 1D). The acquisition of such numerous genomic alterations over the limited growth period of ≤35 generations suggested that these clones likely acquired all CCNAs during a temporally restricted episode of chromosomal instability. The homogeneity of WGS read coverage depths observed in the copy number analyses of these clones supported this conclusion. All CCNAs identified within each clonal population were detected at discrete copy numbers; intermediate levels were not observed (data not shown). This demonstrated that CCNAs did not arise continuously during the expansion of the colony, and instead indicated that the instability underlying the formation of these complex genomic alterations was short-lived.

Models of gradual mutation accumulation predict that the rate at which cells independently lose two chromosomes (2^L) should be the multiplicative product of the rates at which each individual chromosome is lost (1^L), referred to here as the *theoretical* 2^L rate. Our initial results challenged this premise of gradual acquisition and instead suggested that multiple CCNAs could be acquired nonindependently. To quantitatively test this gradual model, we constructed a suite of strains in which jChr5 was marked with two copies of *CAN1* and each of several S288c homologs (sChr1, sChr3, sChr9, sChr12) was marked on both arms with copies of *URA3* (Figure 2A). Plating cultures of these strains to media containing CAN selected for 1^L cells that had lost jChr5, and plating to media containing 5-FOA selected for 1^L cells that had lost the *URA3*-marked homolog (Boeke *et al.* 1984). 2^L cells that had lost both marked homologs were recovered by plating on media containing both CAN and 5-FOA. Notably, neither CAN nor 5-FOA have been found to promote aneuploidization in yeast (Forche *et al.* 2011; Shor *et al.* 2013), and aneuploidies in these clones would necessarily have occurred during the initial culture, prior to exposure to these drugs.

We used fluctuation analysis to determine the rates at which 1^L and 2^L clones arose in ≤35 generation-cultures (Table S8). Consistent with previous reports (Klein 2001; Kumaran *et al.* 2013), 1^L clones arose at rates of 10^{-7}–10^{-6}/division (Figure 2B, yellow bars). Consequently, the *theoretical* 2^L rates for each pair of aneuploidies were exceedingly low (10^{-15}–10^{-13}/division; Figure 2B, black lines). We found that the empirically derived 2^L rates were 600- to 3800-fold higher than these *theoretical* 2^L rates (Figure 2B, striped bars), demonstrating that 2^L clones arise far more frequently than predicted by a gradual model of CCNA acquisition. These results were corroborated by similar experiments in two additional strains (another heterozygous strain S288c/YJM789, and an isogenic strain S288c/S288c; Figure S1 and Table S8), indicating that the higher-than-expected incidence of 2^L clones was a feature common to strains from diverse genetic backgrounds.

In haploids, single aneuploidies (*i.e.*, disomies) can impair chromosomal stability and cause elevated rates of subsequent CCNA acquisition (Sheltzer *et al.* 2011). We considered the possibility that the 2^L clones recovered in our experiments could have resulted from a similar sequential process, and tested whether cells aneuploid for a single chromosome

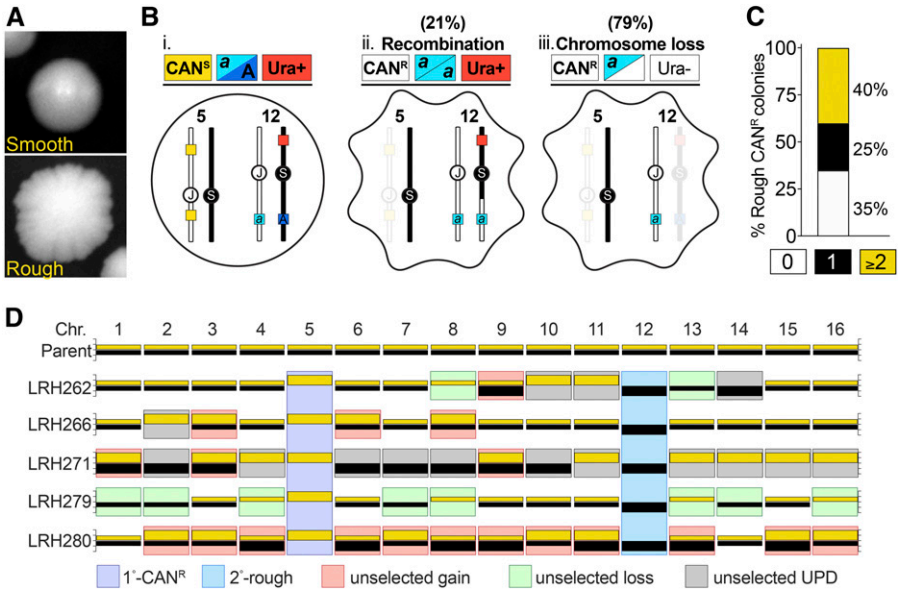

Figure 1 Clones selected for a single CCNA are enriched for additional CCNAs. (A) Images of smooth and rough colonies. (B) A schematic illustrating the genotypic and phenotypic outcomes of selection for loss of jChr5 and homozygosis of *ace2-A7* on jChr12. jChr5-encoded *CAN1* markers, yellow boxes; jChr12-encoded *ace2-A7* mutation, light blue box; sChr12-encoded *ACE2* allele, dark blue box; sChr12-encoded *URA3* marker, red box. (*i*) the parental diploid, (*ii*) 21% of rough CAN^R colonies were Ura$^+$ and homozygous for *ace2-A7* due to MR, (*iii*) 79% of rough CAN^R were Ura$^-$ and hemizygous for *ace2-A7* due to loss of sChr12. (C) Percentage of rough CAN^R isolates with 0 (white), 1 (black), and ≥2 (yellow) unselected CCNAs. (D) Karyotypes of the parent strain and five rough Ura- CAN^R isolates. For each chromosome, yellow bars denote the S288c homolog and black bars denote the JAY291 homolog. Thin bars with a depth equal to those depicted in the parent represent single copies of a given homolog. Thick bars represent two copies of a given homolog. Colored boxes denote the indicated karyotypic events.

exhibited substantially elevated rates of ensuing chromosome loss. If the empirically derived 2^L rates calculated above reflected such a process, then the expected rates at which secondary CCNAs should be acquired would be 1100-fold greater on average (1.2×10^{-4}–1.9×10^{-3}/division, Figure 2C, black lines) than the empirically derived rates of a primary CCNA (Figure 2B, yellow bars). However, we found that 1^L clones (monosomic for sChr1, sChr3, jChr5, or sChr9) lost a second chromosome (jChr5, sChr3, or sChr9) at rates only 2- to 12-fold greater than the euploid parent, and far lower than would be expected if 2^L clones arose through a process of accelerated sequential accumulation (Table S8). Thus, this effect alone cannot explain the high rates at which 2^L clones were recovered in our fluctuation analysis.

We performed WGS analysis of 146 1^L and 2^L isolates, as well as 15 control clones that had been isolated from non-selective conditions (e.g., YPD). We detected no structural abnormalities in the genomes the control clones. By contrast, and in agreement with our earlier results (Figure 1), we again observed a remarkable number of 1^L and 2^L clones harboring additional unselected CCNAs (1^L: 39.0%; 2^L: 47.9%) (Figure 3A). Of these unselected CCNAs, each of the 16 *S. cerevisiae* chromosomes was affected at similar frequencies, and we found no evidence that specific CCNAs co-occurred with any particular selected aneuploidy (Figure 3B). This indicates that unselected CCNAs did not arise subsequently as compensatory suppressors. Additionally, while CCNAs were by far the most prevalent unselected structural genomic alteration, several clones (13/146) had also acquired tracts of LOH resulting from mitotic recombination (Tables S3–S5).

We classified all 146 sequenced clones by the degree to which their genomes had been altered by CCNAs (Figure 3C). Class 1 clones lost only the selected chromosome(s) and represented 58.2% of the dataset (LRH180, 85/146). The remaining 41.8% of clones contained at least one unselected CCNA (61/146) and were classified as follows: Class 2 clones had additionally gained a second copy of the matched homolog resulting in a UPD-type CCNA (LRH183, 21/61, 34.4%); Class 3 clones harbored one additional CCNA (LRH209, 19/61, 31.1%); Class 4 clones harbored multiple additional CCNAs (LRH225, LRH140, LRH187, LRH85, 19/61, 31.1%); and Class 5 clones harbored UPD-type CCNAs of every homolog (LRH11 and LRH159, 2/61, 3.9%).

We also sequenced the genomes of 86 1^L and 2^L isolates derived from the S288c/YJM789 hybrid. Surprisingly, WGS analysis revealed that the parent strain was already trisomic for Chr12 (Figure S2 and Table S5). Despite this pre-existing CCNA, empirically derived 1^L rates for sChr1, sChr3, and yChr5 in this background were comparable to the euploid S288c/JAY291 and S288c/S288c strains (Figure S1 and Table S8). Similar to the clones derived from the S288c/JAY291 hybrid, numerous S288c/YJM789-derived clones contained unselected CCNAs (1^L, 27%; 2^L, 40%) (Table S5). Together, CCNA analysis in this background corroborated our above finding that a single pre-existing CCNA, even of a chromosome as large as Chr12, did not substantially perturb genomic stability, nor did it alter the patterns by which derivative clones acquired unselected CCNAs.

We modeled the number of generations required to produce class 1–5 karyotypes shown in Figure 3C if each CCNA was acquired independently at the average 1^L rate of 1.5×10^{-6}/division (Figure 3D, black dashed line). Contrary to our experimental results, this model projected that class 2–5 karyotypes would have required >35 generations to develop sequentially (41–656 generations) (Figure 3D, yellow circles). Collectively, the conventional gradual model

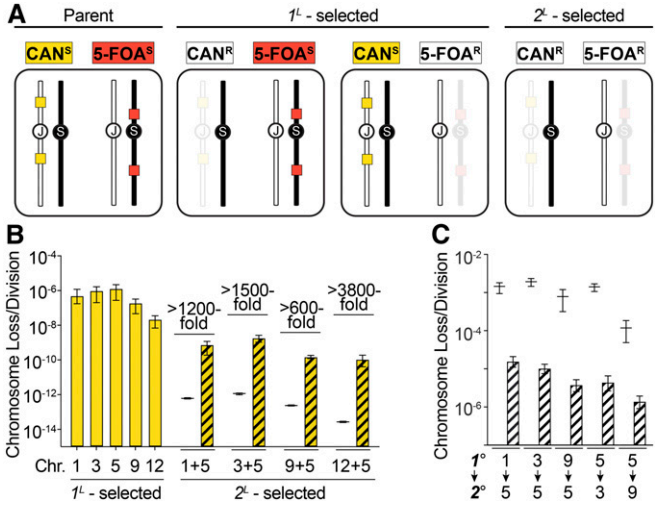

Figure 2 Clones with multiple CCNAs arise more often than predicted by gradual models. (A) Schematic illustrating our quantitative CCNA selection approach. jChr5-encoded *CAN1* markers, yellow boxes, S288c homolog-encoded *URA3* markers, red boxes. (B) Empirically derived rates of each 1^L-selection (yellow) and 2^L-selection (yellow striped). Black lines denote *theoretical* 2^L rates. Fold change between each *theoretical* 2^L rate and empirically derived 2^L rate is noted. (C) Empirically derived rates at which cells with a primary existing CCNA (1°) lose a second chromosome (2°) (striped). Black lines denote the theoretical rates at which each 2°C CNA should occur if 2^L clones arise by sequential acquisition.

does not effectively explain the remarkable genomic complexity detected in clones from the datasets above, nor does it account for the frequency at which we recovered such clones. Instead, our results are best explained by a model in which multiple CCNAs are acquired during a punctuated and transient burst of genomic instability.

Taken together, our results demonstrate the remarkable swiftness with which CCNAs can accumulate to profoundly alter the structure and heterozygosity of a diploid genome. Indeed, cells can and do acquire individual CCNAs independently, indicating that gradual accumulation of CCNAs occurs. But, nearly as often, cells acquire numerous CCNAs coincidentally. This indicates that a broad spectrum of complex karyotypes can arise during stochastic and short-lived episodes, not as the result of gradualism or chronic genomic instability. Our results in *S. cerevisiae* are directly analogous to recent studies that suggest that it is through this punctuated mode of mutagenesis that cancer cells acquire numerous copy number alterations early in tumorigenesis (Gao *et al.* 2016; Casasent *et al.* 2018; Field *et al.* 2018).

For many yeasts, including *S. cerevisiae* and *Candida albicans*, chronic exposure to environmental stresses such as heat- or drug-treatment can rapidly induce *de novo* structural genomic alterations and aneuploidies, which often results in the generation of stress-adapted derivative clones (Hickman *et al.* 2015; Forche *et al.* 2018). For example, exposure of *C. albicans* to the antifungal drug fluconazole is sufficient to increase the rate of whole chromosome aneuploidy by fivefold (Forche *et al.* 2018). Because all aneuploid clones recovered and characterized in this study were isolated from normal growth conditions in rich media, it is unlikely that the punctuated acquisition of CCNAs that we observed can be attributed to stress-induced mutagenesis. Instead, any "stress" that might have promoted aneuploidization of multiple chromosomes simultaneously must have occurred at the single-cell level.

What cellular events might contribute to this process of punctuated copy number evolution (PCNE) (Casasent *et al.* 2018)? Perturbation of many integral cellular processes including DNA damage repair (Craven *et al.* 2002), replication (Wilhelm *et al.* 2019), sister chromatid cohesion (Daum *et al.* 2011; Covo *et al.* 2014), spindle assembly (Mattiuzzo *et al.* 2011; Maiato and Logarinho 2014), and mitotic checkpoint activity (Musacchio 2015) are known to affect the maintenance and inheritance of chromosomes, and failure of any of these pathways has the potential to affect all chromosomes equally and simultaneously (Weaver and Cleveland 2006; Nicholson and Cimini 2011; Musacchio 2015). For instance, even a transient failure to activate the mitotic checkpoint enables a cell to enter anaphase with incorrect chromosome-spindle attachments. Such an erroneous mitosis could produce daughter cells harboring any of the aberrant karyotypic classes described in this study (Figure 3E) (Musacchio 2015). Our experimental approach provides a promising model system with which to meticulously define the causal mechanisms of PCNE as well as to assess the phenotypic consequences and adaptive potential of the remarkable karyotypes that can arise from this process.

Materials and Methods

Strain construction and culture media

All *Saccharomyces cerevisiae* strains used in this study are listed in Supplemental Material, Table S1 and were derived from the S288c, JAY291 (Argueso *et al.* 2009), or YJM789 (McCusker *et al.* 1994) backgrounds. Plasmids used for PCR-based amplification of selectable markers (Wach *et al.* 1994; Goldstein and McCusker 1999; Zhang *et al.* 2013) are listed in Table S2. Strain construction was performed using standard transformation, crossing, and sporulation procedures. Specific descriptions of the construction of experimental strains are outlined below. To ensure that each strain used in these studies was unable to initiate meiosis and undergo a return-to-growth (RTG) process, we replaced the *IME1* locus on each homolog of Chr10 with *HPHMX* selectable markers. RTG is a process in which diploid yeast cells initiate meiotic programs, introduce Spo11-mediated double-strand breaks throughout the genome and then return to vegetative growth (Laureau *et al.* 2016). This process can lead to extensive mitotic recombination-derived loss-of-heterozygosity.

Construction of CAN1-marked chromosomes (jChr5, yChr5, sChr5)

A PCR product consisting of *CAN1-KANMX* amplified from genomic DNA was integrated into the *HOM3* locus on Chr5R.

Resulting strains had the endogenous *CAN1* gene on Chr5L (31694–33466) and the newly introduced *CAN1-KANMX* cassette on Chr5R (256375–257958). Coordinates are derived from the *S. cerevisiae* reference genome build R64-1-1 (yeastgenome.org).

Construction of URA3-marked chromosomes (sChr1, sChr3, sChr9, sChr12)

The *CORE3* cassette (pJA95) encodes tandem *URA3* genes from *S. cerevisiae* (*ScURA3*), *Kluyveromyces lactis* (*KlURA3*) and a *KANMX* cassette. With the exception of Chr1 (see below), the full *CORE3* marker was introduced on the left arm of each S288c chromosome at the coordinate listed in Table S1. Into an isogenic strain of the opposite mating type, a single *KlURA3* marker was inserted into the right arm of the same chromosome at the coordinate listed in Table S1. The two resulting strains were crossed, sporulated, and spores were dissected to recover a haploid derivative with both the left-arm *CORE3* and right-arm *KlURA3* markers. For construction of *URA3*-encoding sChr1, a *KlURA3* marker was inserted into both the left and right arms.

Construction of the TRP1-marked chromosome (sChr3)

To select for loss of sChr3 in the S288c/YJM789 hybrid, the *TRP1* gene was amplified from genomic DNA and integrated into Chr3L and Chr3R at the coordinates listed in Table S1 in the intermediate strains that were used to make sChr1 (above). These strains were then crossed, sporulated, and spores were dissected to recover a haploid derivative encoding both *TRP1* markers and both *KlURA3* markers. This strain was crossed to JAY2593 to form a heterozygous diploid in which chromosomes sChr1, sChr3, and yChr5 were each marked with counter-selectable markers. Although efficacy of *TRP1* counterselection was strong in the S288c/YJM789 genetic background, we found it to be variable in other genetic backgrounds. For example, we discovered that this selection regime was not effective in an SK1-derived background. Due to the variability of counter-selection efficiency, we used only the *URA3* and *CAN1* counterselection regimes for all experiments in the S288c/JAY291 background.

Media used to select CCNA clones

Counterselection of *URA3* was performed by plating cells on synthetic complete media (20 g/liter glucose, 5 g/liter ammonium sulfate, 1.7 g/liter yeast nitrogen base without amino acids, 1.4 g/liter complete drop-out mix, 20 g/liter bacteriological agar) supplemented with 1 g/liter 5-fluoroorotic Acid (5-FOA). Counterselection of *TRP1* was performed by plating cells on synthetic complete media supplemented with 0.75 g/liter 5-fluoroanthranilic Acid (5-FAA). 5-FAA counterselection was only used in plating assays and experiments in the S288c/YJM789 background. Counterselection against *CAN1* was performed by plating cells on synthetic media lacking arginine (20 g/liter glucose, 5 g/liter ammonium sulfate, 1.7 g/liter yeast nitrogen base without amino acids, 1.4 g/liter arginine dropout mix, 20 g/liter bacteriological agar) supplemented with 0.06 g/liter canavanine sulfate (CAN). Selection of 2^L clones was performed by plating cells to appropriate media supplemented with 1 g/liter 5-FOA and 0.06 g/liter CAN, 1 g/liter 5-FOA, and 0.75 g/liter 5-FAA (S288c/YJM789 only), or 0.75 g/liter 5-FAA and 0.06 g/liter CAN (S288c/YJM789 only). Because most S288c chromosomes in the isogenic experiments were marked with *URA3* cassettes, selection of the 2^L combinations sChr1/sChr3, sChr1/sChr9, and sChr1/sChr12 was conducted by plating cells to medium supplemented with 1 g/liter 5-FOA.

Rough colony screening and analysis

Diploid yeast cells of the strain JAY2775 were streaked on solid YPD media and incubated at 30° for 32 hr to allow single colonies to grow. Single colonies were each inoculated into 5 or 7 ml liquid YPD cultures and incubated at 30° for another 24 hr on a rotating drum. Each culture was then diluted appropriately, plated onto CAN-supplemented media, and incubated at 30° for 4 days. Plates were then visually screened for the presence of rough colonies. Rough colonies were isolated with a sterile toothpick and streaked onto both CAN-supplemented media (to preserve a stock) and uracil-dropout media (20 g/liter glucose, 5 g/liter ammonium sulfate, 1.7 g/liter yeast nitrogen base without amino acids, 1.4 g/liter uracil drop-out mix, 20 g/liter bacteriological agar). Plates were incubated at 30° for 24 hr. After 24 hr, each clone was assessed for its ability to grow on uracil-dropout medium.

Genome sequencing and analysis

The genomes of 276 unselected, 1^L, and 2^L clones from either the S288c/JAY291 or S288c/YJM789 hybrid backgrounds were sequenced using Illumina short-read whole-genome sequencing (WGS). Genomic DNA from each clone was isolated using the Yeastar Genomic DNA kit from Zymo Research. Pooled, barcoded libraries of 96 individual genomes were generated using Seqwell plexWell-96 kits. Each 96-sample library was sequenced on a single Illumina HiSeq lane. Using CLC Genomics Workbench software (Qiagen), the following processing pipeline was utilized to analyze each sequenced genome: Illumina reads for each genome were imported into CLC and mapped to the most recent release of the yeast reference genome (R64-2-1, yeastgenome.org). Each resulting read mapping file was then imported into the Nexus Copy Number software (Biodiscovery). Each file was subjected to copy number and single nucleotide polymorphism (SNP) variant analysis to identify the copy number of each chromosome (relative to the diploid parent) and heterozygosity at >20,000 individual sites distributed across the genome. From this, we identified the following structural variations: whole chromosome gains/losses, segmental duplications/deletions, and tracts of (LOH). LOH breakpoints identified in Nexus were confirmed manually in CLC (Tables S3–S5).

Two different approaches were used to define CCNAs, and the analysis of each sequenced dataset are presented in Table S6: (1) the 16-chromosome pairs method; aneuploidy was defined as the deviation of overall ploidy away from 2*n*. Using

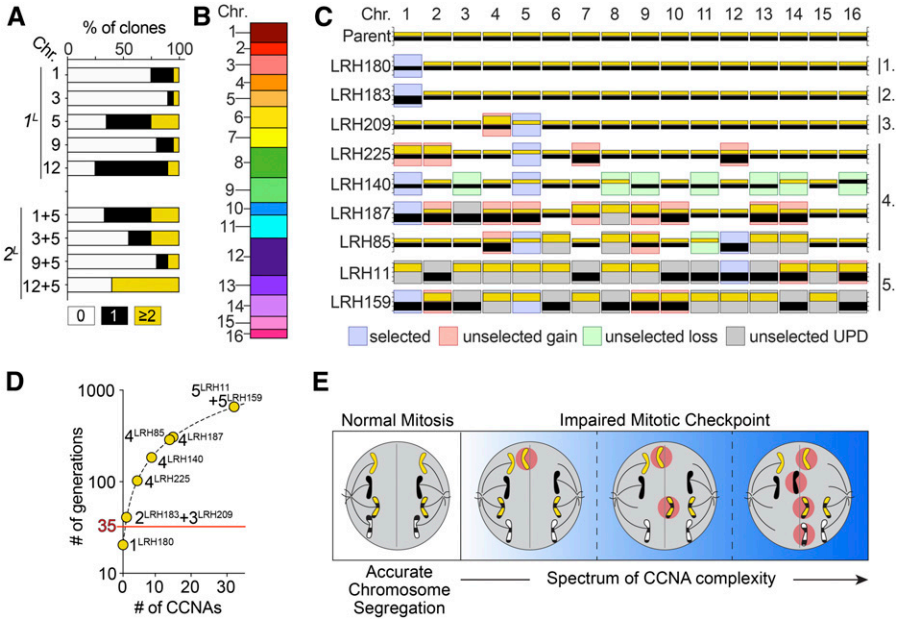

Figure 3 1^L and 2^L clones display a spectrum of CCNA levels. (A) Percentage of 1^L and 2^L isolates with 0 (white), 1 (black), and ≥2 (yellow) unselected CCNAs. (B) Graph depicting the proportion of unselected CCNAs that affected each chromosome. (C) Karyotypes of the parent strain and nine clones representing CCNA classes 1–5. Details as in Figure 1D. (D) Plot depicting a model of gradual CCNA accumulation (black dashed line) and the projected number of generations required to generate class 1–5 clones described in (C) (yellow circles). (E) A model illustrating how mitosis with impaired checkpoint activity could generate cells with varying numbers of CCNAs. Gray line, division plane. Red circles, mis-segregated chromosomes.

this method, uniparental disomy was not scored as an aneuploidy, despite loss of one homolog and gain of the other homolog, (2) the 32-homologs method; aneuploidy was defined as the deviation in copy number of each individual homolog away from 1*n*. Using this method, UPDs were scored as two CCNAs. Graphs in Figures 1C and 3A, and Figure S2A depict the results from the 32-homologs method of analysis. Results from both the 16-chromosome pairs and 32-homologs analyses for each sequenced dataset are presented in Table S6.

Graphs in Figure 3B and Figure S2B depict the proportion of total unselected aneuploidies that affected each yeast chromosome. To determine if there was a bias toward any chromosome in terms of gains/losses, we used the chi-square goodness-of-fit test to compare the distribution of observed frequencies of CCNA for each chromosome to the test distribution of expected frequencies of 6.25% per chromosome (100% divided by 16 chromosomes). From this test, we calculated a *P*-value of 0.109, which indicated that there was no significant difference between each chromosome. Because we found no evidence of biases favoring specific chromosomes, we pooled the total number of unselected aneuploidies in the complete S288c/JAY291 or S288c/YJM789 dataset regardless of primary selection (*e.g.*, selection for loss of sChr1). These data are presented in Table S7.

Quantitative chromosome loss assays

Cultures of S288c/JAY291 diploid strains were prepared from single colonies in a manner identical to that used to select for rough CAN^R clones (see above). Each culture was serially diluted and plated onto YPD (nonselective), 5-FOA- and CAN-supplemented medias (1^L selection), and 5-FOA+CAN-supplemented medium (2^L selection). For the experiments using the S288c/YJM789 diploid strains, cultures were also plated onto 5-FAA-supplemented medium (sChr3 1^L selection), and onto 5-FOA+5-FAA- and CAN+5-FAA-supplemented media (2^L selection). Colonies on nonselective and 1^L-selected plates were counted after 4 days of growth. Colonies on 2^L-selected plates were counted after 6 days of growth. Colony count data were used to calculate rates and 95% confidence intervals of chromosome loss using Flucalc, a MSS-MLE (Ma-Sandri-Sarkar Maximum Likelihood Estimator) calculator for Luria-Delbrück fluctuation analysis (flucalc.ase.tufts.edu) (Radchenko *et al.* 2018). To determine the *theoretical* rates at which 2^L clones should arise if each chromosome was lost independently, the multiplicative product of both observed 1^L rates (and corresponding 95% confidence intervals) was calculated as follows: theoretical rate $2^{L(ChrA+ChrB)}$ = empirically-derived rate $1^{L(ChrA)}$ x empirically-derived rate $1^{L(ChrB)}$. The following rationale was used to calculate the theoretical rates of sequential secondary CCNA acquisition depicted in Figure 2C (black lines). Using empirically-derived 1^L and 2^L rates (Figure 2B and Table S8), we calculated the rate at which a secondary chromosome (ChrB) would be expected to be lost following loss of a primary chromosome (ChrA) if due to sequential process: theoretical sequential rate $1^{L(ChrB)}$ = empirically derived rate $2^{L(ChrA+ChrB)}$/empirically derived rate $1^{L(ChrA)}$. All empirically derived and *theoretical* rates, 95% confidence intervals, and number of cultures used to calculate each rate are listed in Table S8.

Modeling gradual acquisition of CCNAs

We modeled the generations associated with the gradual acquisition of CCNAs using the equation $\#gen = Log_2((1.5 \times 10^6)^{\#A})$ in which #gen equals the number of generations, #A equals number of CCNAs, and 1.5×10^6 defines a representative and constant rate of chromosome loss.

Data availability

The authors state that all data necessary for confirming the conclusions presented in the article are represented fully

within the article. Sequence files for each clone in this study as well as all strains and other data will be shared upon request. Sequence files are also available through NCBI under the BioProject accession number PRJNA657826. Supplemental material available at figshare: https://doi.org/10.25386/genetics.12749273.

Acknowledgments

We are grateful to Eric Alani, Michael McMurray, Dmitry Gordenin, and Tom Petes for valuable comments on the manuscript. This study was supported by National Institutes of Health/National Institute of General Medical Sciences (NIH/NIGMS) awards 1K99GM13419301 to L.R.H. and R35GM11978801 to J.L.A.

Author contributions: Conceptualization: L.R.H. and J.L.A.; Methodology: L.R.H., R.A.W., and J.L.A.; Investigation: L.R.H. and R.A.W.; Resources: J.L.A.; Writing: L.R.H. and J.L.A.; Funding acquisition: J.L.A. and L.R.H. The authors declare no competing interests.

Literature Cited

Andersen, S. L., and T. D. Petes, 2012 Reciprocal uniparental disomy in yeast. Proc. Natl. Acad. Sci. USA 109: 9947–9952. https://doi.org/10.1073/pnas.1207736109

Argueso, J. L., M. F. Carazzolle, P. A. Mieczkowski, F. M. Duarte, O. V. Netto *et al.*, 2009 Genome structure of a Saccharomyces cerevisiae strain widely used in bioethanol production. Genome Res. 19: 2258–2270. https://doi.org/10.1101/gr.091777.109

Boeke, J. D., F. LaCroute, and G. R. Fink, 1984 A positive selection for mutants lacking orotidine-5′-phosphate decarboxylase activity in yeast: 5-fluoro-orotic acid resistance. Mol gen genet. 197: 345–346. https://doi.org/10.1007/BF00330984

Casasent, A. K., A. Schalck, R. Gao, E. Sei, A. Long *et al.*, 2018 Multiclonal invasion in breast tumors identified by topographic single cell sequencing. Cell 172: 205–217.e12. https://doi.org/10.1016/j.cell.2017.12.007

Coelho, M. C., R. M. Pinto, and A. W. Murray, 2019 Heterozygous mutations cause genetic instability in a yeast model of cancer evolution. Nature 566: 275–278. https://doi.org/10.1038/s41586-019-0887-y

Covo, S., C. M. Puccia, J. L. Argueso, D. A. Gordenin, and M. A. Resnick, 2014 The sister chromatid cohesion pathway suppresses multiple chromosome gain and chromosome amplification. Genetics 196: 373–384. https://doi.org/10.1534/genetics.113.159202

Craven, R. J., P. W. Greenwell, M. Dominska, and T. D. Petes, 2002 Regulation of genome stability by TEL1 and MEC1, yeast homologs of the mammalian ATM and ATR genes. Genetics 161: 493–507.

Daum, J. R., T. A. Potapova, S. Sivakumar, J. J. Daniel, J. N. Flynn *et al.*, 2011 Cohesion fatigue induces chromatid separation in cells delayed at metaphase. Curr. Biol. 21: 1018–1024. https://doi.org/10.1016/j.cub.2011.05.032

Eldredge, N., and S. J. Gould, 1972 Punctuated equilibria: an alternative to phyletic gradualism, pp. 82–115 in *Models of Paleobiology,* edited by T. J. M. Schopf. Freeman, Cooper and Co., San Francisco.

Field, M. G., M. A. Durante, H. Anbunathan, L. Z. Cai, C. L. Decatur *et al.*, 2018 Punctuated evolution of canonical genomic aberrations in uveal melanoma. Nat. Commun. 9: 116. https://doi.org/10.1038/s41467-017-02428-w

Forche, A., D. Abbey, T. Pisithkul, M. A. Weinzierl, T. Ringstrom *et al.*, 2011 Stress alters rates and types of loss of heterozygosity in Candida albicans. MBio 2: e00129-11. https://doi.org/10.1128/mBio.00129-11

Forche, A., G. Cromie, A. C. Gerstein, N. V. Solis, T. Pisithkul *et al.*, 2018 Rapid phenotypic and genotypic diversification after exposure to the oral host niche in. Genetics 209: 725–741.

Gao, R., A. Davis, T. O. McDonald, E. Sei, X. Shi *et al.*, 2016 Punctuated copy number evolution and clonal stasis in triple-negative breast cancer. Nat. Genet. 48: 1119–1130. https://doi.org/10.1038/ng.3641

Gilchrist, C., and R. Stelkens, 2019 Aneuploidy in yeast: segregation error or adaptation mechanism? Yeast 36: 525–539. https://doi.org/10.1002/yea.3427

Goldstein, A. L., and J. H. McCusker, 1999 Three new dominant drug resistance cassettes for gene disruption in Saccharomyces cerevisiae. Yeast 15: 1541–1553. https://doi.org/10.1002/(SICI)1097-0061(199910)15:14<1541::AID-YEA476>3.0.CO;2-K

Hickman, M. A., C. Paulson, A. Dudley, and J. Berman, 2015 Parasexual ploidy reduction drives population heterogeneity through random and transient aneuploidy in Candida albicans. Genetics 200: 781–794. https://doi.org/10.1534/genetics.115.178020

Klein, H. L., 2001 Spontaneous chromosome loss in Saccharomyces cerevisiae is suppressed by DNA damage checkpoint functions. Genetics 159: 1501–1509.

Kumaran, R., S. Y. Yang, and J. Y. Leu, 2013 Characterization of chromosome stability in diploid, polyploid and hybrid yeast cells. PLoS One 8: e68094. https://doi.org/10.1371/journal.pone.0068094

Larimer, F. W., D. W. Ramey, W. Lijinsky, and J. L. Epler, 1978 Mutagenicity of methylated N-nitrosopiperidines in Saccharomyces cerevisiae. Mutat. Res. 57: 155–161. https://doi.org/10.1016/0027-5107(78)90262-2

Laureau, R., S. Loeillet, F. Salinas, A. Bergström, P. Legoix-Né *et al.*, 2016 Extensive recombination of a yeast diploid hybrid through meiotic reversion. PLoS Genet. 12: e1005781 (erratum: PLoS Genet. 12: e1005953). https://doi.org/10.1371/journal.pgen.1005781

Loeb, L. A., 2016 Human cancers express a mutator phenotype: hypothesis, origin, and consequences. Cancer Res. 76: 2057–2059. https://doi.org/10.1158/0008-5472.CAN-16-0794

Maiato, H., and E. Logarinho, 2014 Mitotic spindle multipolarity without centrosome amplification. Nat. Cell Biol. 16: 386–394. https://doi.org/10.1038/ncb2958

Mattiuzzo, M., G. Vargiu, P. Totta, M. Fiore, C. Ciferri *et al.*, 2011 Abnormal kinetochore-generated pulling forces from expressing a N-terminally modified Hec1. PLoS One 6: e16307. https://doi.org/10.1371/journal.pone.0016307

McCusker, J. H., K. V. Clemons, D. A. Stevens, and R. W. Davis, 1994 Genetic characterization of pathogenic Saccharomyces cerevisiae isolates. Genetics 136: 1261–1269.

Musacchio, A., 2015 The molecular biology of spindle assembly checkpoint signaling dynamics. Curr. Biol. 25: R1002–R1018 (erratum: Curr. Biol. 25: 3017). https://doi.org/10.1016/j.cub.2015.08.051

Nelson, B., C. Kurischko, J. Horecka, M. Mody, P. Nair *et al.*, 2003 RAM: a conserved signaling network that regulates Ace2p transcriptional activity and polarized morphogenesis. Mol. Biol. Cell 14: 3782–3803. https://doi.org/10.1091/mbc.e03-01-0018

Nicholson, J. M., and D. Cimini, 2011 How mitotic errors contribute to karyotypic diversity in cancer. Adv. Cancer Res. 112: 43–75. https://doi.org/10.1016/B978-0-12-387688-1.00003-X

Nowell, P. C., 1976 The clonal evolution of tumor cell populations. Science 194: 23–28.

Podlaha, O., M. Riester, S. De, and F. Michor, 2012 Evolution of the cancer genome. Trends Genet. 28: 155–163. https://doi.org/10.1016/j.tig.2012.01.003

Radchenko, E. A., R. J. McGinty, A. Y. Aksenova, A. J. Neil, and S. M. Mirkin, 2018 Quantitative analysis of the rates for repeat-mediated genome instability in a yeast experimental system. Methods Mol. Biol. 1672: 421–438. https://doi.org/10.1007/978-1-4939-7306-4_29

Rodrigues Prause, A., N. M. V. Sampaio, T. M. Gurol, G. M. Aguirre, H. N. C. Sedam *et al*., 2018 A case study of genomic instability in an industrial strain of Saccharomyces cerevisiae. G3 (Bethesda) 8: 3703–3713. https://doi.org/10.1534/g3.118.200446

Sampaio, N. M. V., A. Rodrigues Prause, V. P. Ajith, T. M. Gurol, M. J. Chapman *et al*., 2017 Mitotic systemic genomic instability in yeast. bioRxiv (Preprint posted September 17, 2017). https://doi.org/10.1101/161869

Sansregret, L., and C. Swanton, 2017 The role of aneuploidy in cancer evolution. Cold Spring Harb. Perspect. Med. 7: a028373. https://doi.org/10.1101/cshperspect.a028373

Selmecki, A. M., Y. E. Maruvka, P. A. Richmond, M. Guillet, N. Shoresh *et al*., 2015 Polyploidy can drive rapid adaptation in yeast. Nature 519: 349–352. https://doi.org/10.1038/nature14187

Sheltzer, J. M., H. M. Blank, S. J. Pfau, Y. Tange, B. M. George *et al*., 2011 Aneuploidy drives genomic instability in yeast. Science 333: 1026–1030. https://doi.org/10.1126/science.1206412

Shor, E., C. A. Fox, and J. R. Broach, 2013 The yeast environmental stress response regulates mutagenesis induced by proteotoxic stress. PLoS Genet. 9: e1003680. https://doi.org/10.1371/journal.pgen.1003680

The Cancer Genome Atlas Research Network, 2008 Comprehensive genomic characterization defines human glioblastoma genes and core pathways. Nature 455: 1061–1068 [Corrigenda: Nature 494: 506 (2013)]. https://doi.org/10.1038/nature07385

Wach, A., A. Brachat, R. Pöhlmann, and P. Philippsen, 1994 New heterologous modules for classical or PCR-based gene disruptions in Saccharomyces cerevisiae. Yeast 10: 1793–1808. https://doi.org/10.1002/yea.320101310

Weaver, B. A., and D. W. Cleveland, 2006 Does aneuploidy cause cancer? Curr. Opin. Cell Biol. 18: 658–667. https://doi.org/10.1016/j.ceb.2006.10.002

Wilhelm, T., A. M. Olziersky, D. Harry, F. De Sousa, H. Vassal *et al*., 2019 Mild replication stress causes chromosome mis-segregation via premature centriole disengagement. Nat. Commun. 10: 3585. https://doi.org/10.1038/s41467-019-11584-0

Zhang, H., A. F. B. Zeidler, W. Song, C. M. Puccia, E. Malc *et al*., 2013 Gene copy-number variation in haploid and diploid strains of the yeast Saccharomyces cerevisiae. Genetics 193: 785–801. https://doi.org/10.1534/genetics.112.146522

Communicating editor: F. Cole